Global manifolds of vector fields: The general case

Bernd Krauskopf
Dept of Engineering Mathematics
University of Bristol
Bristol BS8 1TR
U.K.
B.Krauskopf@bristol.ac.uk

Hinke Osinga
Control & Dynamical Systems
Caltech 107–81
Pasadena, CA 91125
U.S.A.
hinke@cds.caltech.edu

Revision of September 1999

Abstract

For any $1 < k < n$, we show how to compute the k-dimensional stable or unstable manifold of an equilibrium in a vector field with an n-dimensional phase space. The manifold is grown as concentric (topological) $(k-1)$-spheres, which are computed as a set of intersection points of the manifold with a finite number of hyperplanes perpendicular to the last $(k-1)$-sphere. These intersection points are found by solving a suitable boundary value problem. In combination with a method for adding or removing hyperplanes we ensure that the mesh that represents the computed manifold is of a prescribed quality.

As examples we compute two-dimensional stable manifolds in the Lorenz system and in a four-dimensional Hamiltonian system from optimal control theory.

1 Introduction

In order to understand the global dynamics of vector fields, an important class of models in applications, it is necessary to compute the stable and unstable manifolds of equilibria (or more complicated invariant sets). These global manifolds organize the dynamics: they form boundaries of basins of attraction and are responsible for complicated dynamics and chaos.

Our object of study is a vector field

$$\dot{x} = f(x), \tag{1}$$

with an n-dimensional phase space. For simplicity we assume that $x \in \mathbb{R}^n$ and $f : \mathbb{R}^n \mapsto \mathbb{R}^n$ is sufficiently smooth. We suppose further that $x_0 \in \mathbb{R}^n$

is a hyperbolic saddle point with $(n-k)$ stable and k unstable eigenvalues (counted with multiplicity). The Unstable Invariant Manifold Theorem (Palis & De Melo 1982) guarantees that in a neighborhood of x_0 there exists the local unstable manifold, which is tangent to the unstable (generalized) eigenspace $E^u(x_0)$ of the Jacobian $Df(x_0)$ of (1). Hence, x_0 has the k-dimensional unstable manifold

$$W^u(x_0) \;=\; \{x \in \mathbb{R}^3 \mid \lim_{t \to -\infty} \phi^t(x) = x_0\},$$

where ϕ^t is the flow of (1). Unstable manifolds can generally be found by numerical methods only. (We only compute the unstable manifold; the stable manifold $W^s(x_0)$ can be computed as an unstable manifold by reversing time.)

In this paper we present a general algorithm that computes $W^u(x_0)$ for any $1 < k < n$. The main idea is to grow the manifold by starting with a $(k-1)$-sphere (approximately) in $W^u(x_0)$ close to x_0. In practice, we take a $(k-1)$-sphere in $E^u(x_0)$ close to x_0. Given any $(k-1)$-sphere in $W^u(x_0)$, we find a new $(k-1)$-sphere in $W^u(x_0)$ at a prescribed distance from the old one. To this end, we consider the one-dimensional intersection curves of the k-dimensional unstable manifold with a finite number of $(n-k+1)$-dimensional hyperplanes that are perpendicular to the given $(k-1)$-sphere. This general algorithm is a generalization of the algorithm for the case $k = 2$ and $n = 3$ in Krauskopf & Osinga (1999). (Note that the case $k = 1$ is not considered here, because it boils down to simply integrating an initial condition on $E^u(x_0)$ close to x_0.) The algorithm is now implemented for $k = 2$ and arbitrary n; see the examples in Section 4. We remark that an implementation for $k \geq 3$ will have to deal with serious problems of data management and visualization, which is beyond the scope of this paper. Our algorithm can also be used for the computation of the unstable manifold of an m-torus of saddle type, provided the invariant splitting into linear stable and unstable directions near the torus is known; the latter can be computed using the algorithm in Broer, Osinga & Vegter (1997).

We now briefly discuss other methods for computing unstable manifolds of vector fields; for a more detailed discussion see Krauskopf & Osinga (1999). The idea of growing a $(k-1)$-shpere, which is a circle for $k = 2$, is also used and implemented for $k = 2$ and $n = 3$ in Johnson, Jolly & Kevrekidis (1997) and in Guckenheimer & Worfolk (1993) and Worfolk (1997). The difference with our method is that an initial mesh is evolved by integration. Johnson

et al. update the new mesh by interpolation between mesh points that are too far from each other. This makes it difficult to assess the accuracy of the computation, a problem that may be even more pronounced for $k > 2$. Guckenheimer and Worfolk rescale the vector field so that the tangential component to the last circle is practically zero and the circle is grown in the radial direction by integration. This requires that the rescaled vector field points radially outward everywhere along the last circle, which is why this approach has serious difficulties in the case of complex conjugate eigenvalues. Doedel (1997) computes two-dimensional manifolds by following an orbit of a prescribed arclenth by continuation, where the angle of the orbit with a reference direction near the equilibrium acts as continuation parameter. His method does not seem to allow for a direct generalization to $k > 2$. Dellnitz and Hohmann (1996, 1997) consider the time t map of the flow of (1) for some fixed $t > 0$ and cover the manifold with n-dimensional boxes. A disadvantage is that using the time t map may slow down the computation considerably.

The paper is organized as follows. In Section 2 we give a detailed description of our algorithm. Section 3 contains the proof of correctness. In Section 4 we demonstrate our method by computing two-dimensional stable manifolds in the Lorenz system and in a four-dimensional Hamiltonian system from optimal control theory.

2 The algorithm

We regard the unstable manifold $W^u(x_0)$ as a one-parameter family of (topological) $(k-1)$-spheres, parametrized by arclength from x_0. Our algorithm computes a finite number of such $(k-1)$-spheres, each of which is represented by a finite mesh. Let M_i denote the set of mesh points defining the $(k-1)$-sphere at step i. From the mesh points of M_i we form the simplicial complex S_i, which consists of $(k-1)$-simplices (lines for a 1-sphere, triangles for a 2-sphere, etc.; see Rheinboldt (1998)). Hence, S_i is a piecewise linear continuous approximation of the $(k-1)$-sphere at step i. A first piece of the manifold $W^u(x_0)$ (up to a prescribed arclength) is approximated by the k-dimensional simplicial complex $\mathcal{S}$ which is formed from the total mesh $\mathcal{M} = \cup_i M_i$ in such a way that the $(k-1)$-simplices in S_i appear as faces of the k-simplices of $\mathcal{S}$. This is done in steps by enlarging $\mathcal{S}$ at step i by k-simplices that form the shell between M_i and M_{i+1}.

As starting data M_1 and S_1 we choose a $(k-1)$-sphere in $E^u(x_0)$ at some

prescribed distance δ from x_0. The algorithm now proceeds by adding new $(k-1)$-spheres in steps. Suppose that we have computed M_i and S_i, so that we are at step i in which we want to find M_{i+1} and S_{i+1}. We first find M_{i+1} with the same number of meshpoints as M_i. To this end, we find for every meshpoint $r \in M_i$ a new meshpoint $b_r \in W^u(x_0)$ which lies 'above' r, that is, at a prescribed distance Δ in a direction 'perpendicular' to S_i at r. How this can be done is described in Section 2.1. The collection of these points b_r forms M_{i+1}. Note that the mesh may get extremely distorted if, instead, one integrates the vector field with all $r \in M_i$ as initial conditions to obtain M_{i+1}; compare Johnson *et al.* (1997).

For every point r in M_i we form a curve through r and the corresponding points below it in M_1 through M_{i-1} and above it in M_{i+1}. The key idea is to control the accuracy of the total mesh $\mathcal{M}$ by controlling the accuracy of these curves and that of the meshes M_j of the $(k-1)$-spheres S_j separately. To monitor the accuracy of these one-dimensional curves we use the technique described in Hobson (1993); see Section 2.2 and compare also Krauskopf & Osinga (1998b). To control the accuracy of the $(k-1)$-sphere S_{i+1} meshpoints may need to be added to or removed from M_{i+1}, which is described in Section 2.3. This guarantees the quality of the total mesh $\mathcal{M}$ and also makes it independent of the dynamics.

2.1 Finding a new point in M_{i+1}

Suppose M_i and S_i are known and we are given the point $r \in M_i$. We define an $(n-k+1)$-dimensional hyperplane $\mathcal{F}_r$ with the property that it is 'most perpendicular' to S_i at r. By this we mean that we define $\mathcal{F}_r$ to be perpendicular to suitable averages of the vectors between r and its direct neighbors in M_i. They constitute approximations to the tangent vectors, which are not defined at r since S_i is not differentiable at r. We consider now the intersection of $W^u(x_0)$ with $\mathcal{F}_r$. Note that in the n-dimensional state space the intersection of a k-dimensional manifold with an $(n-k+1)$-dimensional hyperplane is generically a one-dimensional curve. By taking $\mathcal{F}_r$ most perpendicular to S_i at r, we ensure that at least locally near r this curve is well-defined. We are looking for a point b_r that lies on this curve at an appropriate distance Δ from r. The choice of Δ is a guess that is influenced by the local curvature of $W^u(x_0)$. After we find b_r we need to check whether Δ was suitable for the required accuracy; see Section 2.2.

The key idea is that the point $b_r \in \mathcal{F}_r$ can be found by continuing the fol-

lowing boundary value problem until the distance Δ is reached. We consider the orbit $\{ \phi^t(q_r(\tau)) \mid t \in [0,\tau] \}$ satisfying

$$\begin{cases} \phi^0(q_r(\tau)) & \in & S_i, \\ \phi^\tau(q_r(\tau)) & \in & \mathcal{F}_r. \end{cases} \tag{2}$$

We denote the initial condition in S_i by $q_r(\tau)$, and the final point in $\mathcal{F}_r$ by $b_r(\tau) = \phi^\tau(q_r(\tau))$. Note that $b_r(\tau) \in \mathcal{F}_r$ is a point close to $W^u(x_0) \cap \mathcal{F}_r$, because $b_r(\tau)$ lies on an orbit through $q_r(\tau) \in S_i$ which is assumed to be close to $W^u(x_0)$. In fact, the curve $W^u(x_0) \cap \mathcal{F}_r$ is approximated by a curve that is parametrized as $b_r(\tau)$ by the integration time τ. We now define the point $b_r = b_r(\tau_r)$ uniquely by the property that τ_r is the smallest integration time τ for which $\| b_r(\tau) - r \| = \Delta$.

More precisely, we start from the trivial solution $q_r(0) = r$ and $b_r(0) = r$ for $\tau = 0$ which clearly satisfies the boundary condition (2). We then continue this solution in the continuation parameter τ while monitoring the test function

$$\Delta - \| b_r(\tau) - r \| . \tag{3}$$

When we find the first zero of (3) for some $\tau = \tau_r$ the continuation stops and we set $b_r = b_r(\tau_r)$.

2.2 Checking the guess for Δ

After performing the step in the previous section for all $r \in M_i$, we have two $(k-1)$-spheres, namely M_i and M_{i+1}, that each consist of the same number of mesh points. In order to decide whether Δ was appropriate we check the accuracy of the intersection curves through the points $r \in M_i$ and the correspondins points $b_r \in M_{i+1}$. For each of these pairs $r \in M_i$ and $b_r \in M_{i+1}$ there exists a corresponding point $p_r \in M_{i-1}$ that is on the same intersection curve as r and b_r. (We use $M_0 = S_0 = x_0$.) Note that typically $p_r \notin \mathcal{F}_r$; we have $p_r, r \in \mathcal{F}_{p_r}$ and $r, b_r \in \mathcal{F}_r$, and the intersection curve is traced by the piecewise linear curve connecting the three points. Let α_r denote the angle between the line through p_r and r and the line through r and b_r. We accept $\Delta = \| b_r - r \|$ if both

$$\alpha_r < \alpha_{max} , \tag{4}$$

$$\Delta \cdot \alpha_r < (\Delta\alpha)_{max} . \tag{5}$$

If (4) and (5) hold for all $r \in M_i$, we accept M_{i+1} as the next $(k-1)$-sphere. On the other hand, if there is some $r \in M_i$ such that either (4) or (5) is not satisfied then Δ was too big. We discard M_{i+1}, decrease Δ (in practice we halve it), and compute a new M_{i+1} at this smaller distance from M_i.

During the course of the computation Δ is updated as follows. As mentioned above, if Δ was too large then Δ is halved. If Δ was accepted, we usually keep this value of Δ as a guess in the next step. However, if for every $r \in M_i$ both α_r and $\Delta \cdot \alpha_r$ are well below the respective upper bounds, that is, $\alpha_r < \alpha_{min}$ and $\Delta \cdot \alpha_r < (\Delta\alpha)_{min}$ for some prespecified $\alpha_{min} < \alpha_{max}$ and $(\Delta\alpha)_{min} < (\Delta\alpha)_{max}$, then we try a larger Δ in the next step (in practice we double Δ) in order to reduce computation time. The parameters α_{min}, α_{max}, $(\Delta\alpha)_{min}$, and $(\Delta\alpha)_{max}$ control the accuracy of the intersection curves and need to be specified before a computation.

2.3 Adding and removing mesh points

It is very important to have an accurate approximation of S_{i+1} as a subset of $W^u(x_0)$, beause in the $(i+1)$th step S_{i+1} is the approximation of $W^u(x_0)$ used in the formulation of the boundary value problem. Note that the distance between S_i and S_{i+1} does not influence the accuracy of the computation. Already for $k = 3$, it can be quite complicated to construct the simplicial complex S_{i+1} from the set of mesh points M_{i+1}. Here we assume that we have an effective method for obtaining S_{i+1}, so that we only need to worry about the distances between the mesh points in M_{i+1}.

We prespecify minimal and maximal distances between two neighboring mesh points, denoted by $\delta_{\mathcal{F}}$ and $\Delta_{\mathcal{F}}$, respectively. If $\Delta_{\mathcal{F}} <\| b_2 - b_1 \|$ for two neighboring mesh points $b_1, b_2 \in M_{i+1}$ then the mesh is not accurate enough and a new point must be added. We do not simply add an extra point to M_{i+1}, since this would involve interpolation between mesh points in M_{i+1} that are too far apart. Instead, we add a point $\hat{r}$ to M_i by interpolation, which is fine because all mesh points in M_i are within distance $\Delta_{\mathcal{F}}$ from their neighbors. We now determine $\mathcal{F}_{\hat{r}}$ and compute $b_{\hat{r}}$ by solving the corresponding boundary value problem. The point $b_{\hat{r}}$ is now added to M_{i+1} and S_{i+1} is updated locally. We remark that in this step also the k-simplices between S_i and S_{i+1} need to be updated. Note that here lies the main difference in mesh quality control between our approach and those of Guckenheimer & Worfolk (1993), Johnson *et al.* (1997), and Worfolk (1997).

In order to avoid problems with generating S_{i+1} we require that the hy-

perplanes $\mathcal{F}_{b_1}$ and $\mathcal{F}_{b_2}$ of two neighboring mesh points $b_1, b_2 \in M_{i+1}$ do not cross at a distance less than Δ. We ensure this by requiring a minimal distance $\delta_{\mathcal{F}}$ between mesh points of M_{i+1}. If $\| b_2 - b_1 \| < \delta_{\mathcal{F}}$ we delete, say, the mesh point b_1. This has implications for the $(k-1)$-simplices in S_{i+1} near b_1, and also for the k-simplices between S_i and S_{i+1}, which both need to be updated locally. It may happen that this creates a pair of neighboring meshpoints of distance larger than $\Delta_{\mathcal{F}}$, in which case we add a new point according to the procedure above.

It should be clear that local additions to and deletions from M_{i+1} pose complicated problems of updating S_{i+1} and $\mathcal{S}$. This is beyond the scope of this paper for general $1 < k < n$, but it is solved for $k = 2$; see Section 4.

2.4 Convergence to an attractor

With the method described in the previous sections we find $W^u(x_0)$ as the simplicial complex $\mathcal{S}$, parametrized by arclength from x_0. However, if $W^u(x_0)$ has finite arclength, then the arclength typically differs in different directions. In this case we eventually allow for different Δ-steps in different hyperplanes.

Finite arclength in a particular hyperplane $\mathcal{F}_r$ is detected as follows. Recall from Section 2.1 that we continue points $b_r \in \mathcal{F}_r$, parametrized by the integration time τ, while monitoring the test function (3). If $W^u(x_0)$ has finite arclength then (3) may not have a zero. This means that (3) is positive for all $\tau \geq 0$. The point $b_r(\infty)$ (the solution for $\tau \to \infty$) is not part of $W^u(x_0)$, but it is contained in the closure of $W^u(x_0)$. In other words, $b_r(\infty)$ is (part of) an attractor, or an object of saddle type involved in a homoclinic or heteroclinic connection of the unstable manifold $W^u(x_0)$. In practice, an approximation for $b_r(\infty)$ can be found, for example, by monitoring (3) as a function of the integration time τ. If finite arclength in $\mathcal{F}_r$ is detected, an approximation of $b_r(\infty)$ is accepted as the last point and no more points are added in $\mathcal{F}_r$.

3 Correctness

If the mesh parameters δ, Δ, and $\Delta_{\mathcal{F}}$ are taken small enough, the above algorithm produces an approximant of $W^u(x_0)$ up to the prescribed arclength. This approximant will get better and better as the mesh quality is increased. We give an exact statement and proof of this in Theorem 1 for the case that

$W^u(x_0)$ has infinite arclength; the case of a manifold with finite arclength is treated in Corollary 2. For technical reasons we consider a sufficiently large, simply connected compact first finite piece $W^u_{\rm ffp}(x_0) \subset W^u(x_0)$ with $x_0 \in W^u_{\rm ffp}(x_0)$. Furthermore, we assume that $W^u(x_0)$ is a C^2-manifold. Since in practically all applications the vector field is at least C^2, this is not a real restriction.

We use ideas from topology on the convergence of compact connected sets, which are called *continua* (Hocking & Young 1988). See Stuart & Humphries (1996) for a very similar approach in proving the convergence of numerical approximations of attractors to the actual attractor of the underlying continuous dynamical system.

Recall that the usual semi-distance between two sets $A, B, \subset \mathbb{R}^n$ is

$$\begin{aligned} d(A,B) &= \sup_{y\in A}\{d(x,B)\}, \text{ where} \\ d(x,B) &= \inf_{y\in B}\{||x-y||\}. \end{aligned}$$

Let $\mathcal{N}_\varepsilon(X)$ denote the ε-neighborhood of a set $X \subset \mathbb{R}^n$. The Hausdorff distance between two compact sets A and B is defined as

$$\mathrm{d}_{\mathcal{H}}(A,B) = \max\{d(A,B), d(B,A)\},$$

which means that $A \subset \mathcal{N}_\varepsilon(B)$ and $B \subset \mathcal{N}_\varepsilon(A)$.

Let us fix some specific notation. We denote by $\mathcal{S}(\delta,\Delta,l)$ the simplicial complex of arclength l, computed by our algorithm using the accuracy parameters δ and Δ. Here, Δ is the overall mesh quality. In other words, it is assumed that $\Delta_{\mathcal{F}}$ is related to Δ in such a way that $\Delta_{\mathcal{F}} \to 0$ as $\Delta \to 0$, and we take $\Delta_{\mathcal{F}} = \Delta$ for simplicity. Note that $\mathcal{S}(\delta,\Delta,l)$ is a continuum with the property that $x_0 \in \mathcal{S}(\delta,\Delta,l)$. We now fix an arclength L and denote $\mathcal{S}(\delta,\Delta) := \mathcal{S}(\delta,\Delta,L)$. The set of mesh points that defines $\mathcal{S}(\delta,\Delta)$ is denoted by $\mathcal{M}(\delta,\Delta)$, and by construction $\mathcal{M}(\delta,\Delta) \subset \mathcal{S}(\delta,\Delta)$. Recall that the algorithm grows $\mathcal{S}(\delta,\Delta)$ in steps by adding approximations of $(k-1)$-spheres. The mesh points of such a $(k-1)$-sphere at step i are the set $M(\delta,\Delta)_i$ and the corresponding piecewise linear continuous approximation is $S(\delta,\Delta)_i$.

We are interested in the convergence properties of the family $\{\mathcal{S}(\delta,\Delta)\}_{\delta,\Delta}$. Each $\mathcal{S}(\delta,\Delta)$ is a continuum with $x_0 \in \mathcal{S}(\delta,\Delta)$. In order to study convergence we consider the sets

$$\begin{aligned} \mathcal{S}_0^- &= \liminf_{\delta,\Delta\to 0}\{\mathcal{S}(\delta,\Delta)\} = \{x\in\mathbb{R}^n \mid \lim_{\delta,\Delta\to 0} d(x,\mathcal{S}(\delta,\Delta)) = 0\} \text{ and} \\ \mathcal{S}_0^+ &= \limsup_{\delta,\Delta\to 0}\{\mathcal{S}(\delta,\Delta)\} = \{x\in\mathbb{R}^n \mid \liminf_{\delta,\Delta\to 0} d(x,\mathcal{S}(\delta,\Delta)) = 0\}. \end{aligned}$$

In other words, any sequence of approximants with $\delta, \Delta \to 0$ will converge to a continuum containing $\mathcal{S}_0^-$, but may not quite reach $\mathcal{S}_0^+$; compare Stuart & Humphries (1996) and Hocking & Young (1988). Notice that always $\mathcal{S}_0^- \subset \mathcal{S}_0^+$. Furthermore, $\mathcal{S}_0^+$ is a continuum because $x_0 \in \mathcal{S}_0^- \neq \emptyset$.

With this notation we have the following correctness result.

Theorem 1
Fix any simply connected continuum $\mathcal{K} \subset W^u_{\rm ffp}(x_0)$ with $x_0 \in \mathrm{int}(\mathcal{K})$. Then for sufficiently large arclength $L > 0$ we have that $\mathcal{K} \subset \mathcal{S}_0^- \subset \mathcal{S}_0^+ \subset W^u_{\rm ffp}(x_0)$.

Theorem 1 shows that the algorithm correctly computes any fixed continuum $\mathcal{K}$. In fact, we conjecture that $\{\mathcal{S}(\delta, \Delta)\}_{\delta,\Delta}$ converges to a continuum $\mathcal{S}_0 \subset W^u_{\rm ffp}(x_0)$ in the Hausdorff metric as $\delta, \Delta \to 0$. This conjecture is equivalent with proving that $\mathcal{S}_0^- = \mathcal{S}_0^+ =: \mathcal{S}_0$. Proving this is difficult because of the way the mesh changes with δ, Δ: the meshpoints along which the arclength is computed during the computation change in a complicated way with the mesh quality.

Proof of Theorem 1:
The first step in the proof is to show that for any given $\varepsilon > 0$ we have $\{\mathcal{S}(\delta, \Delta)\} \subset \mathcal{N}_\varepsilon(W^u_{\rm ffp}(x_0))$ for sufficiently small δ, Δ, which is upper semicontinuity of $\{\mathcal{S}(\delta, \Delta)\}$ to $W^u_{\rm ffp}(x_0)$. Next we show that there is an arclength L such that $\mathcal{K} \subset \mathcal{N}_\varepsilon(\mathcal{S}(\delta, \Delta))$ for all sufficiently small δ, Δ. This proves that $\mathcal{K} \subset \mathcal{S}_0^-$, which is lower semicontinuity of $\{\mathcal{S}(\delta, \Delta)\}$ to $\mathcal{K}$.

Step 1: upper semicontinuity. The total error $\varepsilon_{\mathcal{S}}$ is defined as

$$\varepsilon_{\mathcal{S}} = d(\mathcal{S}(\delta, \Delta), W^u_{\rm ffp}(x_0)). \tag{6}$$

This means that $\mathcal{S}(\delta, \Delta)$ is contained in $\mathcal{N}_\varepsilon(W^u_{\rm ffp}(x_0))$ for any $\varepsilon > \varepsilon_{\mathcal{S}}$. We obtain upper semicontinuity by showing that $\varepsilon_{\mathcal{S}} \to 0$ as $\delta, \Delta \to 0$.

There are two contributions to the error $\varepsilon_{\mathcal{S}}$. First, the mesh points in $\mathcal{M}(\delta, \Delta)$ do not lie exactly on $W^u(x_0)$, which gives rise to the mesh error

$$\varepsilon_{\mathcal{M}} = d(\mathcal{M}(\delta, \Delta), W^u_{\rm ffp}(x_0)).$$

Second, there is the global interpolation error $\varepsilon_I(\Delta)$ due to the fact that points in $\mathcal{S}(\delta, \Delta) \setminus \mathcal{M}(\delta, \Delta)$ are interpolated linearly. Consequently, we have for the total error

$$\varepsilon_{\mathcal{S}} \leq \varepsilon_{\mathcal{M}} + \varepsilon_I(\Delta). \tag{7}$$

Note that, unlike in the error analysis of the approximation of an implicitly defined invariant manifold (Rheinboldt 1998), these two errors are not independent. The interpolation error at step i enters into the mesh error at step $i+1$. Hence, if we wish to compute more accurate mesh points we need to start an entirely new computation with higher accuracy.

Note that the interpolation error $\varepsilon_I(\Delta)$ goes to zero with Δ, so that in light of (7) it suffices to show that $\varepsilon_{\mathcal{M}}$ goes to zero. To this end, we define the mesh error at step i

$$\varepsilon_{\mathcal{M}}(i) = d(M(\delta,\Delta)_i, W^u_{\rm ffp}(x_0)).$$

The inital mesh error $\varepsilon_{\mathcal{M}}(1)$ is due to the fact that $M(\delta,\Delta)_1$ is chosen in the linear subspace $E^u(x_0)$ at distance δ from x_0, instead of on $W^u(x_0)$. By taking δ small, $\varepsilon_{\mathcal{M}}(1)$ can be made arbitrarily small. Under the assumption that $W^u(x_0)$ is C^2, the initial error $\varepsilon_{\mathcal{M}}(1)$ is of order $O(\delta^2)$.

The mesh error $\varepsilon_{\mathcal{M}}(i+1)$ at step $i+1$ can be estimated in terms of $\varepsilon_{\mathcal{M}}(i)$ as follows. Points in $M(\delta,\Delta)_{i+1}$ are found by continuing the boundary value problem (2). Since the accuracy of the boundary value solver is indepedent of the other computational errors, we assume that solving the boundary value problem does not introduce an extra error. Recall that, for any $r \in M(\delta,\Delta)_i$, the starting point of the boundary value problem (2) is denoted by $q_r(\tau_r) \in S(\delta,\Delta)_i$ and the end point by $b_r(\tau_r) \in \mathcal{F}_r$, where τ_r is the integration time such that $\| b_r(\tau_r) - r \| = \Delta$. The error at $S(\delta,\Delta)_{i+1}$ comes from the fact that $S(\delta,\Delta)_i$ is only approximately on $W^u(x_0)$, so that we are solving the 'wrong' boundary value problem. Therefore,

$$\begin{aligned}\varepsilon_{\mathcal{M}}(i+1) &= \max_{r\in M(\delta,\Delta)_i} d(b_r(\tau_r), W^u_{\rm ffp}(x_0)) \\ &= \max_{r\in M(\delta,\Delta)_i} d(\phi^{\tau_r}(q_r(\tau_r)), W^u_{\rm ffp}(x_0)). \qquad (8)\end{aligned}$$

Since $W^u_{\rm ffp}(x_0)$ is compact, we may assume that the vector field satisfies a Lipschitz condition in a neighborhood U of $W^u_{\rm ffp}(x_0)$. This means that

$$d(\phi^t(p), W^u_{\rm ffp}(x_0)) \le e^{\kappa_U t}\, d(p, W^u_{\rm ffp}(x_0)) \qquad (9)$$

for some constant κ_U, and such that the orbit of p up to $\phi^t(p)$ is in U; see also Stuart & Humphries (1996). Combining this with (8) and defining τ_i such that $e^{\kappa_U \tau_i} = \max\limits_{r\in M(\delta,\Delta)_i} (e^{\kappa_U \tau_r})$, we get

$$\begin{aligned}\varepsilon_{\mathcal{M}}(i+1) &\le \max_{r\in M(\delta,\Delta)_i} e^{\kappa_U \tau_r} d(q_r(\tau_r), W^u_{\rm ffp}(x_0)) \\ &\le e^{\kappa_U \tau_i}\, \varepsilon_{\mathcal{S}}(i) \le e^{\kappa_U \tau_i}\, (\varepsilon_{\mathcal{M}}(i) + \varepsilon_I(\Delta)). \qquad (10)\end{aligned}$$

The local manifold is always an attractor (Palis & De Melo 1982), so there exists a neighborhood $V \subset U$ of x_0 on which we find a Lipschitz constant $\kappa_V < 0$. By choosing δ sufficiently small we can assure that $S(\delta,\Delta)_1 \subset V$. Suppose that the first, say, J spheres lie in V, that is, $S(\delta,\Delta)_i \subset V$ for $1 \leq i \leq J$. We then have

$$\varepsilon_{\mathcal{M}}(i+1) \leq e^{\kappa_V \tau_i}(\varepsilon_{\mathcal{M}}(i) + \varepsilon_I(\Delta)) \leq \varepsilon_{\mathcal{M}}(1) \quad \text{for} \quad 1 \leq i < J, \tag{11}$$

provided Δ is small enough.

We now show that the error on $U \setminus V$ can be controlled. For the $(k-1)$-spheres in $U \setminus V$ of which there are, say, N, using (10) and the fact that $\kappa_U > 0$ we get

$$\begin{aligned} \varepsilon_{\mathcal{M}}(J) &\leq \cdots \leq \varepsilon_{\mathcal{M}}(N+J) \\ &\leq e^{\kappa_U \bar{\tau}} \varepsilon_{\mathcal{M}}(1) + N e^{\kappa_U \bar{\tau}} \varepsilon_I(\Delta)\,. \end{aligned} \tag{12}$$

Here, the number $\bar{\tau}$ is chosen such that $\sum_{i=J}^{N+J-1} \tau_i \leq \bar{\tau}$. In fact, $\bar{\tau}$ is an upper bound on the total integration time that is needed by the algorithm to cover $U \setminus V$, which depends only on the prescribed arclength (once V is fixed). In other words, $\bar{\tau}$ can be chosen such that it is independent of N. By combining (11) and (12) we have

$$\begin{aligned} \varepsilon_{\mathcal{M}} &= \max_{1 \leq i \leq N+J} \{\, \varepsilon_{\mathcal{M}}(i) \,\} \\ &= \max\{\, \varepsilon_{\mathcal{M}}(1), \varepsilon_{\mathcal{M}}(N+J) \,\} \\ &\leq e^{\kappa_U \bar{\tau}} \varepsilon_{\mathcal{M}}(1) + N e^{\kappa_U \bar{\tau}} \varepsilon_I(\Delta))\,. \end{aligned} \tag{13}$$

The term $e^{\kappa_U \bar{\tau}} \varepsilon_{\mathcal{M}}(1)$ in (13) can be made arbitrarily small by decreasing δ. In order to make the term $N e^{\kappa_U \bar{\tau}} \varepsilon_I(\Delta)$ in (13) arbitrarily small $\varepsilon_I(\Delta)$ needs to decrease faster than linear with Δ. This is guaranteed by the assumption that $W^u(x_0)$ is at least C^2, in which case $\varepsilon_I(\Delta) = O(\Delta^2)$. It follows that $\varepsilon_{\mathcal{S}} \to 0$ as $\delta, \Delta \to 0$, which concludes step 1.

Step 2: lower semicontinuity. Consider a fixed simply connected continuum $\mathcal{K} \subset W^u_{\rm ffp}(x_0)$ with $x_0 \in \mathrm{int}(\mathcal{K})$. We need to show that, for any $\varepsilon > 0$, $\mathcal{K} \subset \mathcal{N}_\varepsilon(\mathcal{S}(\delta,\Delta))$, for δ and Δ small enough.

Because $x_0 \in \mathrm{int}(\mathcal{K})$ and $\mathcal{K}$ is compact, we can find an n-dimensional topological ball $B \subset V$ around x_0 such that $W_B(x_0) := \mathcal{K} \cap B$ is an overflowing manifold that intersects ∂B in exactly a topological $(k-1)$-sphere. We also assume that B is so small that $W^u_{\rm ffp}(x_0) \cap B = \mathcal{K} \cap B$, which is possible because $W^u_{\rm ffp}(x_0)$ is compact. By construction of B, $\mathcal{S}(\delta,\Delta)$ intersects ∂B in

a topological $(k-1)$-sphere for all sufficiently small δ, provided the arclength L is chosen large enough. But then the lim inf and the lim sup of the family $\{\mathcal{S}(\delta,\Delta)\cap\partial B\}_{\delta,\Delta}$ are equal. As a consequence, using step 1, we have that $\{\mathcal{S}(\delta,\Delta)\cap B\}_{\delta,\Delta}$ converges to $W_B(x_0)$ in the Hausdorff metric as $\delta,\Delta\to 0$; compare Hocking & Young (1988) and Stuart & Humphries (1996).

Because $\partial\mathcal{K}\subset W^u_{\rm fp}(x_0)$, every point of $\partial\mathcal{K}$ is connected by a trajectory to a unique point on the set $\partial W_B(x_0)\subset\partial B$. Let us now fix an $x\in\partial\mathcal{K}$ and let $y:=\phi^{-t(x)}(x)\in\partial W_B(x_0)$, which defines the integration time $t(x)$. We now choose a fixed $\bar\varepsilon$ small enough so that for all $z\in\mathcal{N}^{cl}_{\bar\varepsilon}(x)$ there is a (first) $t(z)>0$ with

$$\phi^{-t(z)}(z)\in\partial B.$$

Here $\mathcal{N}^{cl}_{\bar\varepsilon}(x)$ is the closure of the ε-neighborhood $\mathcal{N}_{\bar\varepsilon}(x)$. This ensures that the set

$$R(y):=\{\phi^{-t(z)}(z)\mid z\in\mathcal{N}^{cl}_{\bar\varepsilon}(x)\}$$

is a simply connected closed neighborhood in ∂B of the unique point $y\in\partial W_B(x_0)$. The set

$$\Phi(\mathcal{N}^{cl}_{\bar\varepsilon}(x)):=\{\phi^{-t}(z)\mid z\in\mathcal{N}^{cl}_{\bar\varepsilon}(x)\text{ and }t\in[0,t(z)]\}$$

is a flowbox, that is, a topological cylinder of some definite minimal diameter.

Consider now two points y_1 and y_2 in the interior of the two different components of $R(y)\setminus\partial W_B(x_0)$. Their two trajectories $\Phi(y_i):=\{\phi^t(y_i)\mid t\in[0,t(y_i)]\}$ in $\Phi(\mathcal{N}^{cl}_{\bar\varepsilon}(x))$ are at a minimal distance, say, η from $\mathcal{K}\cap\Phi(\mathcal{N}^{cl}_{\bar\varepsilon}(x))$ and from the trajectory of the boundary of $R(y)\subset\partial B$, that is, from the side walls of the flow box. By construction of B this means that

$$d(\Phi(y_i),\mathcal{K})\geq\eta.$$

Suppose now that $\delta,\Delta<\eta$ are such that $d(\mathcal{S}(\delta,\Delta)\cap R(y),\partial W_B(x_0)\cap R(y))<\eta$ (and that the arclength L is large enough). We now assume that $\mathcal{S}(\delta,\Delta)\cap\mathcal{N}^{cl}_{\bar\varepsilon}(x)=\emptyset$. This means that $\mathcal{S}(\delta,\Delta)$ may 'enter' the flowbox $\Phi(\mathcal{N}^{cl}_{\bar\varepsilon}(x))$ at $R(y)$ but it cannot 'exit' it on the other end. We know from the flowbox property that a mesh point of $\mathcal{S}(\delta,\Delta)$ is in $\Phi(\mathcal{N}^{cl}_{\bar\varepsilon}(x))$ if and only if also the initial condition of the corresponding boundary value problem is in $\Phi(\mathcal{N}^{cl}_{\bar\varepsilon}(x))$. Moreover, $\mathcal{S}(\delta,\Delta)$ must have mesh points in $\Phi(\mathcal{N}^{cl}_{\bar\varepsilon}(x))$ because $\Delta<\eta$, which is less than the minimal diameter of $\Phi(\mathcal{N}^{cl}_{\bar\varepsilon}(x))$. As the algorithm builds up $\mathcal{S}(\delta,\Delta)$, the flowbox property ensures that the mesh

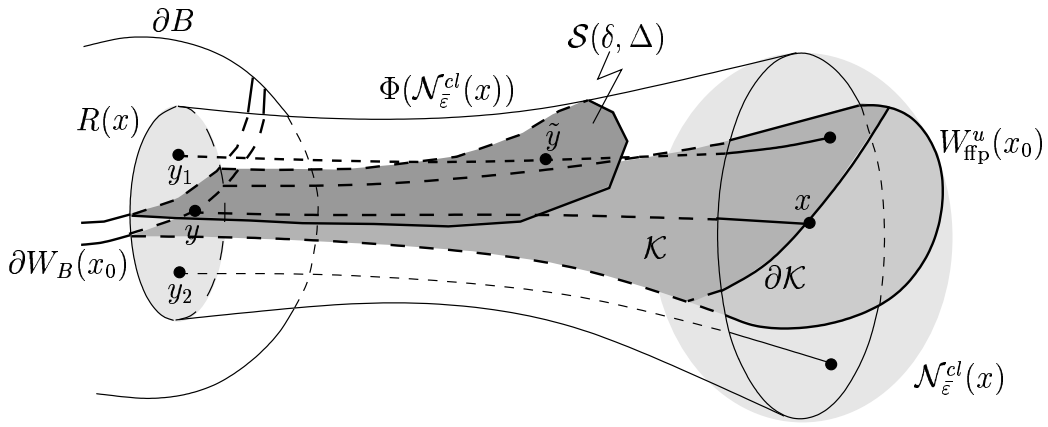

Figure 1: *Sketch in* $\mathbb{R}^3$ *of the situation that* $\mathcal{S}(\delta,\Delta)$ *leaves the flow box* $\Phi(\mathcal{N}_{\bar{\varepsilon}}^{cl}(x))$*; see step 2 in the proof of Theorem 1 for details.*

points of $\mathcal{S}(\delta,\Delta)$ that are in $\Phi(\mathcal{N}_{\bar{\varepsilon}}^{cl}(x))$ come closer and closer to $\mathcal{N}_{\bar{\varepsilon}}^{cl}(x)$ unless $\mathcal{S}(\delta,\Delta)$ leaves $\Phi(\mathcal{N}_{\bar{\varepsilon}}^{cl}(x))$ beforehand via its side walls, as is sketched in Figure 1. This is possible because we make an interpolation error. However, if $\mathcal{S}(\delta,\Delta)$ cuts through a side wall of $\Phi(\mathcal{N}_{\bar{\varepsilon}}^{cl}(x))$, then there is a point $\tilde{y} \in \mathcal{S}(\delta,\Delta) \cap \Phi(y_i)$. In other words, we found a point $\tilde{y} \in \mathcal{S}(\delta,\Delta)$ at distance at least η from $\mathcal{K}$.

In step 1 we showed that for all δ, Δ small enough, the distance of any point in $\mathcal{S}(\delta,\Delta)$ to $W^u_{\mathrm{ffp}}(x_0)$ will be less than $\eta > 0$. Since $W^u_{\mathrm{ffp}}(x_0) \cap \Phi(\mathcal{N}_{\bar{\varepsilon}}^{cl}(x)) = \mathcal{K} \cap \Phi(\mathcal{N}_{\bar{\varepsilon}}^{cl}(x))$, we conclude from the reasoning above that $\mathcal{S}(\delta,\Delta)$ must intersect $\mathcal{N}_{\bar{\varepsilon}}^{cl}(x)$, for all sufficiently small δ, Δ.

In conclusion, we have shown that for any point x_t in the backward orbit $\Phi(x)$ of $x \in \partial\mathcal{K}$ there is a point of $\mathcal{S}(\delta,\Delta)$ in $\mathcal{N}_\varepsilon(x_t)$ for all $\varepsilon > 0$ and sufficiently small δ, Δ. Because $\Phi(x)$ is compact we can choose, for each $x \in \partial\mathcal{K}$, uniform largest δ_x, Δ_x such that

$$\mathcal{S}(\delta,\Delta) \cap \mathcal{N}_\varepsilon(\Phi(x)) \neq \emptyset \quad \text{for all } \delta < \delta_x \text{ and } \Delta < \Delta_x.$$

Since $\partial\mathcal{K}$ is compact, we can choose $\delta_\mathcal{K}$ and $\Delta_\mathcal{K}$ such that

$$\mathcal{S}(\delta,\Delta) \cap \mathcal{N}_\varepsilon(\cup_{x\in\partial\mathcal{K}}\Phi(x)) \neq \emptyset \quad \text{for all } \delta < \delta_\mathcal{K} \text{ and } \Delta < \Delta_\mathcal{K}.$$

Because $\mathcal{K} \setminus W_B(x_0) \subset \cup_{x\in\partial\mathcal{K}}\Phi(x)$ this shows that

$$\mathcal{K} \subset \mathcal{N}_\varepsilon(\mathcal{S}(\delta,\Delta)) \quad \text{for all } \delta < \delta_\mathcal{K} \text{ and } \Delta < \Delta_\mathcal{K},$$

which concludes step 2 by definition of $\mathcal{S}_0^-$. □

Corollary 2
If $W^u(x_0)$ has finite arclength then the family $\{\mathcal{S}(\delta,\Delta)\}_{\delta,\Delta}$ converges to the continuum $(W^u(x_0))^{cl}$ in the Hausdorff metric as $\delta,\Delta \to 0$, provided the specified arclength L is sufficiently large.

Proof of Corollary 2:
Because $W^u(x_0)$ has finite arclength the set $\mathcal{A} := \partial W^u(x_0)$ is a smooth attractor of dimension at most $k-1$. Therefore, there is an $\tilde{\varepsilon}$ such that the vector field admits a Lipschitz condition (see (9)) with a negative Lipschitz constant on the $\tilde{\varepsilon}$-neighborhood $\mathcal{N}_{\tilde{\varepsilon}}^{cl}(\mathcal{A})$. Consider the continuum

$$\mathcal{K}_1 := W^u(x_0) \cap \mathcal{N}_{\tilde{\varepsilon}}^{C}(\mathcal{A}),$$

where $\mathcal{N}_{\tilde{\varepsilon}}^{C}(\mathcal{A})$ denotes the complement of $\mathcal{N}_{\tilde{\varepsilon}}(\mathcal{A})$ in $\mathbb{R}^n$. The proof of Theorem 1 still holds with the minor modification that convergence is detected along leaves; see Section 2.4. Therefore, we conclude that $\mathcal{K}_1 \subset S_0^- \subset S_0^+ \subset W^u(x_0)$. As before, this implies that $\{\mathcal{S}(\delta,\Delta) \cap \mathcal{N}_{\tilde{\varepsilon}}^{C}(\mathcal{A})\}_{\delta,\Delta}$ converges to $\mathcal{K}_1$ in the Hausdorff metric as $\delta,\Delta \to \infty$.

Consider now the continuum

$$\mathcal{K}_2 := (W^u(x_0))^{cl} \cap \mathcal{N}_{\tilde{\varepsilon}}^{cl}(\mathcal{A}).$$

Since we took L large enough, $\mathcal{S}(\delta,\Delta)$ intersects $\mathcal{N}_{\tilde{\varepsilon}}^{cl}(\mathcal{A})$ in a $(k-1)$-sphere. Inside $\mathcal{N}_{\tilde{\varepsilon}}^{cl}(\mathcal{A})$ we have a negative Lipschitz constant, so that $(W^u(x_0))^{cl}$ is an attracting set. As before, we conclude that the family $\{\mathcal{S}(\delta,\Delta) \cap \mathcal{N}_{\tilde{\varepsilon}}^{cl}(\mathcal{A})\}_{\delta,\Delta}$ converges to $\mathcal{K}_2$ in the Hausdorff metric as $\delta,\Delta \to 0$.

Combining the two results completes the proof. □

An example of a two-dimensional unstable manifold of finite arclength converging to an attracting limit cycle can be found in (Krauskopf & Osinga 1999). We finally remark that it is not possible to compute a priori error bounds. For example, there is no method for estimating the Lipschitz constants κ_V and κ_U. To check the accuracy of a computation in practice one should recompute the manifold with increased accuracy and compare the results.

4 Examples

The algorithm is presently implemented for manifolds of dimension $k = 2$ in a state space of arbitrary dimension n. In this case the manifold $W^u(x_0)$ is parametrized by a family of (topological) circles M_i. The 1-simplices that form the continuous objects S_i are line segments between neighboring points in M_i. The simplicial complex $\mathcal{S}$ representing $W^u(x_0)$ consists of triangles that constitute the shells between consecutive circles M_{i-1} and M_i. The algorithm grows $W^u(x_0)$ by adding a new circle to $\mathcal{M}$ at each step, which means that a new shell or ring of triangles of width Δ is added to $\mathcal{S}$.

The boundary value problem (2) is solved with a shooting approach, for which we use a fixed time step Runge-Kutta order four integration routine. The alternating bands in Figures 2 and 3 are the rings that are added at each step. The width of each ring depends on the curvature of the manifold locally near the ring. The figures have been rendered with Geomview (Phillips, Levy & Munzner 1993). See `http://www.fen.bris.ac.uk/engmaths/research/reports/99r15/` for color stills and animations of the growth process.

4.1 The Lorenz system

We first demonstrate our algorithm for a two-dimensional manifold in a three-dimensional phase space, so that there are no problems with viewing the results. To this end, we consider the well-known Lorenz system (Lorenz 1963) on $\mathbb{R}^3$, defined as

$$\begin{cases} \dot{x} &= \sigma(y - x) \\ \dot{y} &= \varrho x - y - xz \\ \dot{z} &= xy - \beta z. \end{cases} \tag{14}$$

For the parameters we choose $\sigma = 10$, $\varrho = 28$, and $\beta = 0.4$, in which case an attracting periodic orbit encircles two saddle points. The origin is a third saddle point and Figure 2(a) shows its two-dimensional stable manifold $W^s(0)$.

The manifold $W^s(0)$ was computed with the following accuracy. The computation started with 20 points on a circle in $E^s(0)$ of radius $\delta = 1.0$ around the origin. Then new circles were added at distances Δ controlled by $\alpha_{min} = 0.3$, $\alpha_{max} = 0.4$, $(\Delta\alpha)_{min} = 0.1$, and $(\Delta\alpha)_{max} = 1.0$; see Sections 2.1 and 2.2. (For practical reasons a new circle was always accepted if $\Delta \leq 0.01$.)

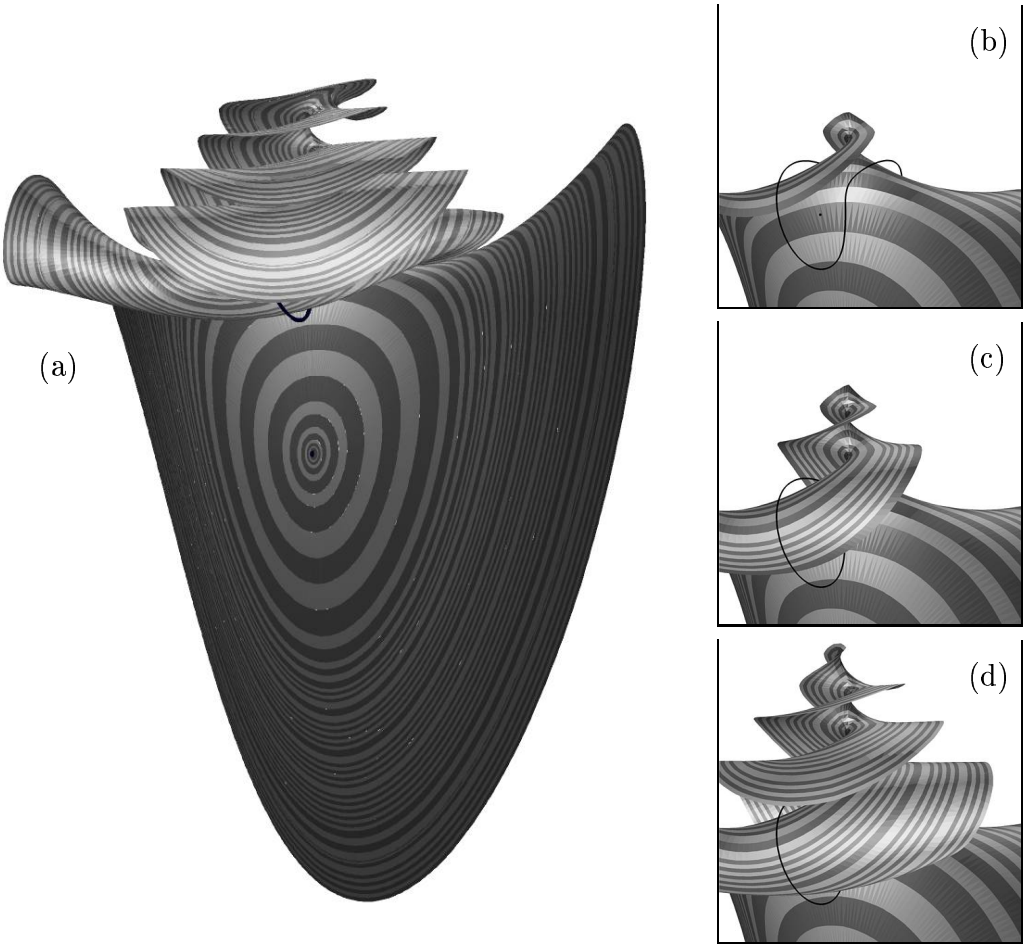

Figure 2: *The stable manifold $W^s(0)$ of the Lorenz system for $\sigma = 10$, $\varrho = 28$, and $\beta = 0.4$, computed up to arclength 66.28 (a). Close-ups near the attracting periodic orbit show the growth process: 25 rings or arclength 40.25 (b), 35 rings or arclength 46.25 (c), and 50 rings or arclength 54.75 (d).*

The mesh points on a circle are never more than $\Delta_{\mathcal{F}} = 1.0$ and less than $\delta_{\mathcal{F}} = 0.25$ apart. In total 75 circles were computed on $W^s(0)$; the last circle is approximately at arclength 66.28 from the origin, and it consists of 1522 mesh points. How $W^s(0)$ is grown during the computation is shown in Figure 2(b)-(d) with three close-up views near the attracting periodic orbit.

4.2 An optimal control system

The following example from optimal control theory is taken from Jadbabaie, Yu & Hauser (1999) and demonstrates that our implementation for $k = 2$ can indeed be used in ambient spaces of arbitrary dimension. Consider an inverted planar pendulum balancing on a cart. The cart moves in the plane of the pendulum with an applied horizontal force u constituting a control. The mass of the cart is M, the mass of the pendulum m and its center of mass is at distance l from the pivot. Disregarding the model equations associated with the cart gives the two-dimensional vector field

$$\begin{cases} \dot{x_1} &= x_2 \\ \dot{x_2} &= f(x_1, x_2) + c(x_1, x_2)u \\ &:= \dfrac{\frac{g}{l}\sin(x_1) - \frac{1}{2}m_r x_2^2 \sin(2x_1) - \frac{m_r}{ml}cos(x_1)u}{\frac{4}{3} - m_r \cos^2(x_1)}. \end{cases} \tag{15}$$

Here x_1 is the angle measured from the vertical up position, $m_r = m/(m+M)$ is the mass ratio, and g is the gravitational constant. Note that the origin is an unstable equilibrium corresponding to the vertical position above the pivot.

We wish to find an optimal control u as a function of x_1 and x_2 that drives the system to the origin, while minimizing the cost function

$$Q(x_1, x_2, u) = \mu_1 x_1^2 + \mu_2 x_2 + \mu_u u^2. \tag{16}$$

Pontryagin's maximum principle (Van der Schaft 1994) ensures that an optimal solution exists and is represented by special solutions of the four-dimensional Hamiltonian system given by the Hamiltonian:

$$\begin{aligned} H(x_1, x_2, p_1, p_2) &= Q(x_1, x_2, u^*(x_1, x_2, p_1, p_2)) + p_1 x_2 + \\ &\quad p_2\, f(x_1, x_2) + p_2\, c(x_1, x_2)\, u^*(x_1, x_2, p_1, p_2), \end{aligned} \tag{17}$$

where $u^*(x_1, x_2, p_1, p_2) = -\frac{1}{2\mu_u}\, c(x_1, x_2) p_2$. One is particularly interested in the geometrical properties of the two-dimensional stable manifold of the

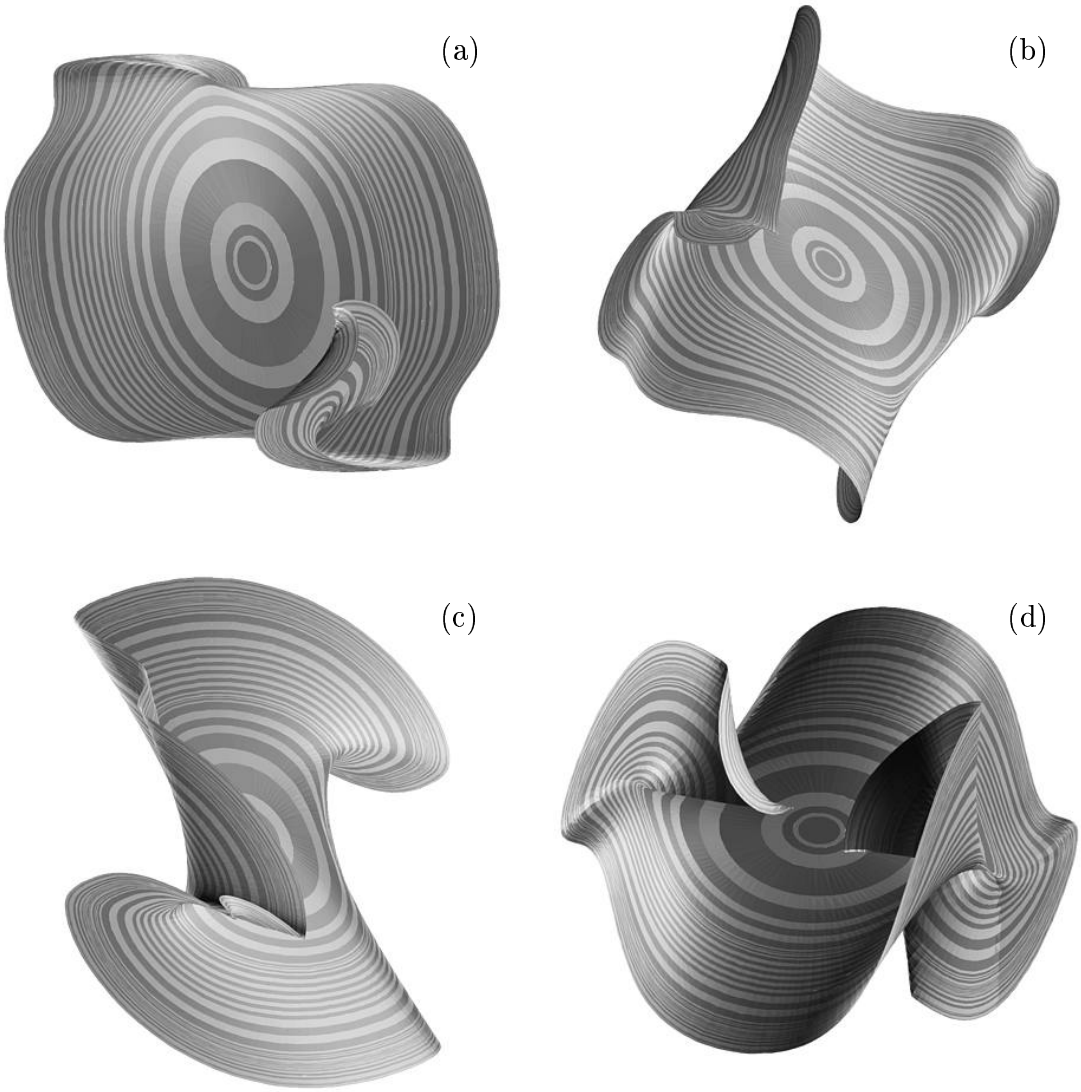

Figure 3: *Four views of the two-dimensional stable manifold $W^s(0)$ up to arclength 16.5 of system (17) projected onto the three-dimensional spaces $\{p_2 = 0\}$ (a), $\{p_1 = 0\}$ (b), $\{x_2 = 0\}$ (c), and $\{x_1 = 0\}$ (d). The self-intersections in (d) are due to the projection.*

origin, because $u^*(x_1, x_2, p_1, p_2)$ is the optimal control achieving the minimum for the cost function (16) provided (x_1, x_2, p_1, p_2) lies on $W^s(0)$. If there is more than one point on $W^s(0)$ for given x_1 and x_2, then there exists more than one optimal control that drives (x_1, x_2) to the origin in (15) with the same minimal cost.

We computed $W^s(0)$ using the parameter values as in Jadbabaie *et al.* (1999), namely $m = 2\,\mathrm{kg}$, $M = 8\,\mathrm{kg}$, $l = 0.5\,\mathrm{m}$, $g = 9.8\,\mathrm{m/s^2}$, $\mu_1 = 0.1$, $\mu_2 = 0.05$ and $\mu_u = 0.01$. We used the following accuracy parameters for the computation. The starting data was a set of 20 points on a circle in $E^s(0)$ of radius $\delta = 1.0$ around the origin. The distance Δ at which new circles were added was controlled by $\alpha_{min} = 0.3$, $\alpha_{max} = 0.4$, $(\Delta\alpha)_{min} = 0.05$, $(\Delta\alpha)_{max} = 0.2$, where we always accepted the circle if $\Delta \leq 0.05$; see Sections 2.1 and 2.2. The distances between mesh points on a circle were always in between $\delta_{\mathcal{F}} = 0.125$ and $\Delta_{\mathcal{F}} = 0.5$. The computed arclength is approximately 16.5, using 65 circles. The last circle has 481 mesh points. Because the ambient space is four-dimensional it is difficult to view the result. In Figure 3 we show four views in four different three-dimensional projections. Note that the optimal control $u^*(x_1, x_2, p_1, p_2) = -\frac{1}{2\mu_u} c(x_1, x_2)\, p_2$ does not depend on p_1. Therefore, the folds shown in the projection onto $\{p_1 = 0\}$ in Figure 3 (b) indicate that indeed more than one optimal control exists for a set of (x_1, x_2) values.

5 Conclusions

We described a general algorithm for computing the global k-dimensional stable or unstable manifold of an equilibrium in an n-dimensional vector field, for any $1 < k < n$. It can also be used to compute the stable or unstable manifold of an invariant m-torus, provided this m-torus and an approximation of its linear stable and unstable directions can be found; for a method to compute the latter we refer to Broer *et al.* (1997).

We showed that our algorithm is correct. It approximates a first piece of the unstable manifold with a given error that goes to zero as the tolerance parameters of the algorithm go to zero. Hence, the approximants are upper semicontinuous to $W^u(x_0)$. We also proved lower semicontinuity to any compact simply connected manifold $\mathcal{K} \subset W^u(x_0)$ with $x_0 \in \mathrm{int}(\mathcal{K})$ provided the arclength is chosen large enough. As a corollary we get Hausdorff convergence if $W^u(x_0)$ has finite arclength.

The algorithm has been implemented for the case $k = 2$ and arbitrary n; see the examples in Section 4. In this situation the two-dimensional manifold is approximated by a simplicial complex consisting of triangles. We note that $n \geq 4$ requires visualizing a two-dimensional object in a high-dimensional space; see Section 4.2.

Already the implementation of the case $k = 3$ (for $n = 4$ or any $n \geq 4$) is of much greater complexity and remains work for the future. The unstable manifold is then approximated by a set of 2-spheres, which are represented by simplicial complexes S_i consisting of triangles. The shells between neighboring 2-spheres consist of tetrahedra, which results in more complex overall data management. Moreover, one encounters the general problem of visualizing a three-dimensional object in a four-dimensional space. This makes it difficult to communicate the results, even though some packages, for example Geomview (Phillips *et al.* 1993), allow to inspect three-dimensional manifold data.

Acknowledgments

B.K. is grateful for a travel grant from The Royal Society and for hospitality and support of the Control and Dynamical Systems Department at the California Institute of Technology, Pasadena. H.O. was supported by AFOSR/DDRE MURI grant AFS-5X-F496209610471; she acknowlegdes the hospitality of the Engineering Mathematics Department at Bristol University and thanks A.M. Stuart for a thorough discussion of an earlier manuscript. We also thank the anonymous referee for pointing out the possibility to proof a stronger result.

References

BROER, H.W., OSINGA, H.M., & VEGTER, G. 1997 Algorithms for computing normally hyperbolic invariant manifolds. *Z. angew. Math. Phys.* **48**, 480–524.

DELLNITZ, M., & HOHMANN, A. 1996 The computation of unstable manifolds using subdivision and continuation. In *Nonlinear Dynamical Systems and Chaos* (Broer, H.W., Van Gils, S.A., Hoveijn, I., & Takens, F. eds.), *PNLDE* **19** Birkhäuser, 449–459.

DELLNITZ, M., & HOHMANN, A. 1997 A subdivision algorithm for the computation of unstable manifolds and global attractors. *Num. Math.* **75**, 293–317.

DOEDEL, E.J. October 1997 Private communications at the IMA, Minneapolis.

GUCKENHEIMER, J., & WORFOLK, P. 1993 Dynamical systems: Some computational problems. In *Bifurcations and Periodic Orbits of Vector Fields* (Schlomiuk, D. ed.) Kluwer Academic Publishers, 241–277.

HOBSON, D. 1993 An efficient method for computing invariant manifolds of planar maps. *J. Comput. Phys.* **104**(1), 14–22.

HOCKING, J.G., & YOUNG, G.S. 1988 *Topology* Dover Publications.

JADBABAIE, A., YU, J., & HAUSER, J. 1999 Unconstrained receding horizon control: stability and region of attraction results. to appear in *IEEE Proc. Conf. Decision & Control.*

JOHNSON, M.E., JOLLY, M.S., & KEVREKIDIS, I.G. 1997 Two-dimensional invariant manifolds and global bifurcations: some approximation and visualization studies. *Numerical Algorithms* **14**, 125–140.

LORENZ, E.N. 1963 Deterministic nonperiodic flows. *J. Atmospheric Sci.* **20**, 130–141.

KRAUSKOPF, B. & OSINGA, H.M. 1998a Globalizing two-dimensional unstable manifolds of maps. *Int. J. Bif. Chaos* **8**(3), 483–503.

KRAUSKOPF, B. & OSINGA, H.M. 1998b Growing 1D and quasi 2D unstable manifolds of maps. *J. Comp. Phys.* **146**(1), 404–419.

KRAUSKOPF, B. & OSINGA, H.M. 1999 Two-dimensional global manifolds of vector fields. *CHAOS* **9**(3), 768–774.

PALIS, J., & DE MELO, W. 1982 *Geometric Theory of Dynamical Systems.* Springer, Heidelberg.

PHILLIPS, M., LEVY, S., & MUNZNER, T. 1993 Geomview: An Interactive Geometry Viewer. *Notices of the Amer. Math. Soc.* **40**, 985–988. This software and the accompanying manual are available at `http://www.geom.umn.edu/`.

RHEINBOLDT, W.C. 1998 *Methods for Solving Systems of Nonlinear Equations* (Second Edition). CBMS-NSF Regional Conference Series in Applied Mathematics **70**, SIAM Publications, Philadelphia.

STUART, A.M., & HUMPHRIES, A.R. 1996 *Dynamical Systems and Numerical Analysis.* Cambridge University Press.

VAN DER SCHAFT, A.J. 1994 *L_2-Gain and Passivity Techniques in Nonlinear Control.* Lecture Notes in Control and Information Sciences **218**, Springer, London.

WORFOLK, P. May 1997 Private communications at the Geometry Center, Minneapolis.